Minos-mediated transgenesis in the pantry moth *Plodia interpunctella*

Short title: Minos transgenesis in *Plodia* pantry moths

Donya N. Shodja[1,*], Luca Livraghi[1], Arnaud Martin[1,*]
1. Department of Biological Sciences, The George Washington University, Washington, DC, USA
* Corresponding authors, e-mail addresses: donya.shodja@gwu.edu ; arnaud@gwu.edu

Abstract

Transposon-mediated transgenesis has been widely used to study gene function in Lepidoptera, with *piggyBac* being the most commonly employed system. However, because the *piggyBac* transposase originates from a lepidopteran genome, it raises concerns about endogenous activation, remobilization, and silencing of transgenes , thus questioning its suitability as an optimal tool in Lepidoptera. As an alternative, we evaluated the dipteran-derived *Minos* transposase for stable germline transformation in the pantry moth, *Plodia interpunctella*. We injected syncytial embryos with transposase mRNA, along with donor plasmids encoding *3xP3::EGFP* and *3xP3::mCherry* markers of eye and glial tissues. Across multiple experiments, we found that G_0 injectees could transmit *Minos* transgenes through the germline even in the absence of visible marker expression in the soma, and that large mating pools of G_0 founders consistently produced transgenic offspring at efficiencies exceeding 10%. Using these methods, we generated transgenic lines with a dual expression plasmid, using *3xP3::mCherry* for driving red fluorescence in eyes and glial tissues, as well as the *Fibroin-L* promoter expressing the recently developed mBaoJin fluorescent protein in the silk glands. This demonstrated the feasibility of screening two pairs of promoter activity in tissues of interest. Collectively, these results—along with previous findings in the silkworm *Bombyx mori*—demonstrate that *Minos* achieves robust germline integration of transgenes in Lepidoptera, offering a valuable pathway to the genetic modification of species where the remobilization or suppression of *piggyBac* elements might be rampant.

Introduction

There is growing interest in developing new laboratory model systems and methods for the study of functional genomics in Lepidoptera, an enormous insect lineage where the silkworm *Bombyx mori* has been a focal species for the study of gene function. The pantry moth *Plodia interpunctella* is a pest of stored food with life history traits that make it suitable for economical and long-term maintenance of genetic lines. We and others have previously established methods for non-homologous repair mediated CRISPR mutagenesis, CRISPR short edits based on homologous recombination, and *piggyBac*-mediated transgenesis in this organism (Bossin et al. 2007; Heryanto, Mazo-Vargas, et al. 2022; Heryanto, Hanly, et al. 2022; Shirk et al. 2023). So far, we have failed to insert a transgenic cassette of several kilobases using CRISPR-related techniques based on homologous repair and non-homologous plasmid insertion. Transposon-based random insertion of transgenes thus

remains a valuable method in *Plodia*, and we expect that the further optimization of such methods will potentiate fundamental studies of lepidopteran biology, notably because the reagents used in these experiments—the source of transposase mRNA and the transgene donor plasmids—are easy to transfer to new species without modification.

One potential limitation of transgenesis in Lepidoptera as currently implemented, however, is that the favored *piggyBac* transposase originated from a lepidopteran species, the cabbage looper *Trichoplusia ni* (Fraser et al. 1985). Several distant lepidopteran species are known to harbor nearly identical *piggyBac* elements in their genomes, raising concern that their endogenous activity could elicit remobilization of newly inserted cassettes (Zimowska and Handler 2006; Wu et al. 2008; Wang et al. 2010). Consistent with these potential issues, two studies documented that *piggyBac* transgenes can be remobilized in *Bombyx* and hinder the interpretability of reporter assays (Wang et al. 2015; Jia et al. 2021). In addition, certain species could have evolved silencing mechanisms to limit *piggyBac* element invasion and transmission (Zimowska and Handler 2006), as characterized in *Drosophila* flies that evolved resistance to P-element transposons (Khurana et al. 2011; Teixeira et al. 2017; Moon et al. 2018). Given these potential concerns, it is important to assess whether transposons originating from more distant lineages work with a similar efficiency in Lepidoptera.

Here we investigated the suitability of an alternative transposon-based method using the *Minos* transposase. *Minos* is a *Tc1/mariner* element derived from the dipteran *Drosophila hydei* that has has been widely used for transgenesis in insects (Franz and Savakis 1991; Loukeris et al. 1995; Loukeris et al. 1995; Kapetanaki et al. 2002; Pavlopoulos et al. 2004; Metaxakis et al. 2005), and other invertebrates (Zagoraiou et al. 2001; Hozumi et al. 2010; Kontarakis and Pavlopoulos 2014; Jackson et al. 2024; Kuo et al. 2024). Importantly, a previous study found that the *Minos* transposase can mediate efficient germline integration in *Bombyx* embryos when delivered as an *in vitro* transcribed mRNA (Uchino et al. 2007). We transferred these methods to *Plodia,* observed efficient germline transmission of two plasmids, validated the expression of three fluorescent markers, and overall, confirmed that *Minos* can mediate stable transgenesis in another lepidopteran laboratory system. We discuss strategies for the rapid generation of transgenic lines in *Plodia* and provide detailed methods to facilitate the use of this technique in other species.

Material & Methods

Plasmids

The *pMi[3xP3::EGFP-SV40]* donor plasmid and the *Minos* transposase transcription template plasmid *pBlueSKMimRNA* (Pavlopoulos et al. 2004) were sourced from Addgene (*RRID:Addgene_102540; RRID:Addgene_102535*). The *pMi[3xp3::mCherry-SV40, Plodia-FibL::mBaojin-P10]* plasmid was produced using Gibson Assembly, by replacing the *EGFP-SV40* section of *pMi[3xP3::EGFP-SV40]* with a synthetic (*mCherry-SV40, FibL::mBaoJin-P10)* gene fragment synthesized by Twist Bioscience, and is available from Addgene (*RRID:Addgene_240410*).The FibL promoter sequence corresponds to 1 kb of sequence upstream of the *P. interpunctella FibL* gene (NCBI: LOC128678647).

Preparation of *Minos* transgenesis reagents

Plasmids were amplified in 50 mL liquid cultures of Luria-Bertani broth with 100 µg/mL Ampicillin, and plasmid DNA was purified with the ZymoPURE II Plasmid Midiprep Kit (Cat# D4200). Plasmids were eluted in 120 µL of elution buffer, yielding concentrations >4,800 ng/µL of plasmid DNA.

To produce *Minos* transposase mRNA, the *pBlueSKMimRNA* plasmid was linearized using the *Not*I-HF restriction enzyme (New England Biolabs), purified by gel extraction using the Zymoclean Gel DNA Recovery Kit (Zymo Research), and further purified using the Zymo DNA Clean & Concentrator-25 kit with an elution volume of 13 µL of DNA elution butter. Subsequently, the HiScribe T7 ARCA mRNA with tailing kit (New Englands Biolabs) was used for transcription and capping of *Minos* transposase mRNA, followed by purification using the MEGAClear Transcription Clean-Up Kit (Thermo Fisher Scientific). The purified mRNA was eluted in 50 µL of the provided elution buffer, which was pre-heated to 65°C and incubated on the filter column for 10 minutes in a 65°C oven. After quantification with Nanodrop (Thermo Fisher Scientific), the transposase mRNA was divided into > 520 ng/µL one-time use aliquots and stored at -70°C.

Injection mixes were freshly prepared before injection and consisted of 400 ng/µL *Minos* transposase mRNA, 200 ng/µL donor plasmid, and 0.05% Phenol Red (1:10 dilution of a 0.5% cell-culture grade Phenol Red solution, Sigma-Aldrich), brought to a 5 µL final volume with 1x *Bombyx* injection buffer (pH = 7.2, 0.5 mM NaH_2PO_4, 0.5 mM Na_2HPO_4, 5 mM KCl).

***Plodia* strain**

The white-eyed *wFog* laboratory strain of *Plodia interpunctella* was used to facilitate the screening of *3xP3*-driven fluorescence in pupal and adult eyes (Heryanto, Hanly, et al. 2022; Heryanto, Mazo-Vargas, et al. 2022). This strain consists in the genome background of the *Dundee* strain (NCBI genome accession GCA_900182495.1), into which a *white* gene *c.737delC* mutation originating from the *Piw3* strain (NCBI genome accession: GCA_022985095.1) was introgressed during two generations of backcrossing and several rounds of sib-sib inbreeding (Heryanto, Hanly, et al. 2022).

***Plodia* husbandry**

The *wFog* strain and the transgenic broods were reared in the laboratory from egg to adulthood in an incubator set at 28°C with 40-70% relative humidity and a 14:10 h light:dark cycle, following methods made available via the Open Science Framework repository (Heryanto et al. 2025). Briefly, egg laying was induced by CO_2 narcosis of adult stocks in an oviposition jar, and a weight boat containing 10-13 mg eggs was placed in a rearing container containing 45-50 g of wheat bran diet with 30% glycerol (**Table S1**). This life cycle spans 29 days from fertilization to a reproductively mature adult stock at 28°C.

Microinjection of *Plodia* syncytial embryos

The general procedure for microinjection as well as a list of suggested equipment is available online (Heryanto, Mazo-Vargas, et al. 2022) and summarized below. *Minos* capped mRNA and the donor plasmid were mixed into a 5 µL aliquot (400 : 200 ng/µL mRNA:DNA) and kept on ice shortly before the procedure. Eggs were collected in an oviposition jar following CO_2

narcosis of a stock of *wFog* strain adults, aligned on parafilm, and microinjected between 20-50 min after egg laying (AEL) using borosilicate pulled glass needles and an air pressure microinjector. Eggs were then sealed with cyanoacrylate glue and left to develop at 25°C or 28°C in a closed tupperware with a wet paper towel.

Fluorescent screening equipment

All life stages were screened under an Olympus SZX16 stereomicroscope equipped with a Lumencor SOLA Light Engine SM 5-LCR-VA lightsource, mounted to a trinocular tube connected to an Olympus DP73 digital color camera. Fluorophore expression was observed using Chroma Technology filter sets ET-EGFP 470/40x 510/20m (GFP) and AT-TRITC-REDSHFT 540/25X, 620/60m (RFP). Autofluorescence patterns are shown for uninjected individuals, using the GFP and RFP filter sets and exposure times consistent with the other images in this study (**Fig. S1**). It is worth adding that a YFP filter set (e.g. Chroma ET-EYFP 500/20x 535/30m) reduces cuticle autofluorescence and can be advantageous to use in addition to a GFP filter set for screening *EGFP* and *mBaoJin* expression. For small mosaic clones, or weak fluorescent signals, the YFP filter on its own may lead to false negatives.

Screening of embryos and first instars larvae

To obtain synchronized embryos, mated adults are anesthetized by CO_2 narcosis and transferred to a glass jar with a mesh lid insert (Heryanto et al. 2025). CO_2 exposure triggers egg release in *Plodia*, and embryos are collected after 2-4 hrs,transferred to a glass petri dish, and incubation at 28°C and saturating humidity (*e.g.* in a sealed tupperware with a wet paper towel), until time of screening. The screening of embryos is most convenient when using crosses performed in relatively large pools, for example with more than 10 mated females. Screening of transgenic embryos is optimal at 68-74h h after egg laying (AEL) if incubated at 28°C, a time window where *3xP3*-driven fluorescence in presumptive glia and ocelli is discernible in the larval head and body. Earlier times of screening show weaker fluorescence and confounding signals, likely due to the episomal expression of residual plasmids in large vitellophages (Heryanto, Mazo-Vargas, et al. 2022). Hatching occurs at 78-82 h AEL in uninjected embryos and can be delayed by up to 12 h in G_0 embryos, due to injection stress.

Screening of pupae and adults

The screening of pupae is ideal to verify the transgenic status of imagos in preparation of a new generation, and can also be the method of choice when screening offspring from small crosses (less than 10 females), where isolating synchronized embryos by CO_2 narcosis is not optimal. As pupae can be difficult to isolate from the larval diet, it is helpful to add strips of cardboard to larval containers that contain fifth instar larvae, as the corrugations within this material are the preferred pupation site that facilitates the collection of pupae (Shim and Lee 2015). Pupae are then isolated from these lodges, as well as from those located within the diet, transferred to tissue culture dishes for screening and sex sorting, and subsequently combined according to the cross design in fresh containers to allow adult emergence and mating prior to initiating the next generation. Fluorescent and brightfield images of pupae

were acquired using the same fluorescent microscopy set-up using the Olympus DP74 camera, and overlaid using the Screen blending mode in Adobe Illustrator. Brightfield images of transgenic G_2 adult eyes (**Fig. 1F**) were taken using a Keyence VHX-5000 digital microscope. Pupal stages (%, **Fig. 1C, 2G**) were estimated based on eye, wing, tarsal, and cuticle pigmentation (Zimowska et al. 1991). Adult moths can be screened in a petri dish held on ice to limit moth activity.

Characterization of silk gland fluorescence

The *FibL::mBaojin* transgene drives strong silk gland fluorescence visible directly through the cuticle of all larval instars. The silk glands of a G_2 *FibL::mBaojin* transgenic fifth instar larva were dissected, fixed, and mounted following a previously described procedure (Alqassar and Martin 2025), and imaged on an Olympus SZX16 fluorescence stereomicroscope, as well as on an Olympus FV1200 confocal microscope mounted with a 20x objective.

Results

Somatic and germline transformation of a test *Minos* donor plasmid

To test for the efficacy of *Minos*-mediated transgenesis in *Plodia* embryos, we initially microinjected 1,317 eggs between 20-50 mins after egg laying (AEL), with the *pMi[3xP3::EGFP-SV40]* test donor plasmid (Pavlopoulos et al. 2004). This injection time window, as well as the microinjection technique and rearing conditions were comparable to our previous experiments using the *Hyperactive piggyBac* transposase (*HyPBase*) in *Plodia* (Heryanto, Mazo-Vargas, et al. 2022). The injection mix consisted of capped poly-A tailed *Minos* mRNA, mixed with a donor plasmid for the integration of the *3xP3::EGFP* transgenesis marker cassette.

We conducted three injection trials using the *pMi[3xP3::EGFP-SV40]* plasmid. All three attempts resulted in detectable activity in a portion of G_0 embryos and pupae. Embryonic activity of *3xP3::EGFP*, observed as of bright fluorescent puncta in the presumptive glia and larval ocelli (Thomas et al. 2002; Bossin et al. 2007; Heryanto, Mazo-Vargas, et al. 2022; Pearce et al. 2024), was respectively detected in 10.3%, 7.8% and 4.3% of G_0 embryos in Experiments #1, #2 and #3 (**Fig. 1A, Table 1**). Pupal activity of *3xP3::EGFP*, consisting of bright fluorescent stripes of expression in the pupal eyes of the *wFog* white-eyed strain used here (Heryanto, Mazo-Vargas, et al. 2022), was observed in 7.1%, 15.7%, and 16.7% of pupae in Experiments #1, #2 and #3 (**Fig. 1B, Table 1**). Overall, these data indicate that *Minos* transposase can drive transgene insertion into the genome of somatic cells.

Next, we assessed whether *Minos* could efficiently transpose the test insert into the germline, and enable its transmission over subsequent generations. Following Experiment #1, we in-crossed all the 14 G_0 adults by pooling them for random mating and rearing in a single container. We recovered 250 G_1 pupae, 23.6% of which showed transgene activity (**Fig. 1C, Table 2**). Following Experiment #2, we similarly in-crossed 41 G_0 adults, but then directly screened embryos instead of pupae. This in-cross generated 470 G_1 embryos, of which 11.5% were transgenic (**Table 2**). It is worth noting that in these two crosses, 13 out of 14 of the G_0 founders from Experiment #1, and all of the G_0 founders from Experiment #2, lacked a

detectable somatic activity of *3xP3::EGFP* at the pupal stage. For comparison, we out-crossed 5 EGFP$^+$ G_0 males from Experiment #2 to 10 females from the uninjected *wFog* strain, and obtained 10.6% transgenic embryos out of 113 G_1 eggs. In summary, both G_0 negative and positive individuals can be used as founders for germline transmission of *Minos* transgenes, as somatic transformants do not necessarily reflect whether germline transformation has occurred.

Stable transgene transmission over several generations

Further examination of the germline-integrate *3xP3::EGFP* transgene activity revealed fluorescence patterns identical to the ones previously reported with *piggyBac*-mediated integration (Heryanto, Mazo-Vargas, et al. 2022), consistent with glial expression in embryos, and ocelli expression in larvae (**Fig. 1D-E, Video S1**). In the depigmented eyes from the *wFog* strain, the retinal expression of EGFP was strong enough to reveal a green tint of the eyes, visible without fluorescent microscopy equipment (**Fig. 1F**).

In addition, out of the 59 G_1 pupae with eye fluorescence generated from Experiment #1, 10 showed an additional, unexpected fluorescence in pupal oenocytes (Stendell 1912; Shirk and Zimowska 1997; Makki et al. 2014), visible as ventral metameric belts in the second to seventh abdominal segments (**Fig. 1C', Fig. S2**). This activity is likely due to an identical insertion shared between these 11 siblings. Below we refer to this randomly captured oenocyte activity as coming from a single *EGFP*$^{+/oeno}$ allele, and dub the transgene alleles that lack it *EGFP*$^+$. To further test the transmissibility of these G_1 insertion alleles, we generated four crosses each consisting of a single *EGFP*$^+$ or EGFP$^{+/oeno}$ G_1 founder mixed with four non-transgenic individuals from the opposite sex. These crosses generated 60.2% transgenic G_2 offspring individuals on average (**Table 2**), including transmission of the *EGFP*$^{+/oeno}$ allele in the two corresponding crosses.

We then continued these experiments over the G_3 and G_4 generations to further assess transgene stability **(Table 2)**. To obtain G_3 offspring, we performed two backcrosses each consisting of one positive G_2 female mixed with 4 non-transgenic white-eyed males, yielding 51.3% [*EGFP*$^+$] G_3 pupae in the first cross, and 46.0% [*EGFP*$^{+/oeno}$] pupae in the second cross, each consistent with their donor parent carrying a single copy of a EGFP$^+$ or EGFP$^{+/oeno}$ insertion allele (Chi-square test $p > 0.7$; no significant deviation from 50% transmission). Pooled in-crossing of positive G_3 individuals yielded 100% G_4 positive progeny in both cases, with [*EGFP*$^+$] or [*EGFP*$^{+/oeno}$] fluorescent expression patterns consistent with their G_2 donor grand-parent. The persistence of ectopic oenocyte activity across four generations suggests that the location of the expression cassette was stable and had not been subjected to re-transposition.

The *FibL* promoter enables fluorescent marking of the silk glands

Next, to provide an alternative marker to eye/glia in future experiments, we designed a new donor plasmid aimed at labeling the silk glands. In *Bombyx*, the promoter of the *Fibroin-L* silk gene (*FibL*) drives fluorescent protein expression in the posterior region of the silk glands, enabling detection through the cuticle. This promoter has notably been used as a transgenesis marker in experiments where the labeling of neural tissues is unwanted (Imamura et al. 2003; Fujiwara et al. 2014). To implement a similar strategy, we cloned a 1 kb

fragment of the *Plodia FibL* proximal promoter to drive the expression of *mBaoJin*— a recently developed monomeric fluorophore with remarkable brightness and photostability (Zhang et al. 2024) followed by a P10 3'UTR sequence (Xu et al. 2022). This cassette was cloned upstream of a *3xP3::mCherry* red fluorescence eye marker in order to monitor successful integrations.

Injections of the resulting *Minos* donor plasmids yielded positive hatchling larvae and pupae expressing distinguishable mosaic patches of *3xP3::mCherry* expression in the eye/glia (**Fig. 2A, 2B**). We conducted 2 independent injections trials using this plasmid, Experiments #4 and #5). Experiments #4 generated only one somatic transformant out of 77 pupae (**Table 1**), and random in-crossing of this large pool of founders successfully generated transgenic 22 transgenic G_1 larvae, out of more than a hundred screened larvae (we failed to record an exact number of screened larvae, and can not provide a germline transmission rate in this experiment). These G_1 individuals successfully transmitted transgenes into G_2 backcrosses in a pattern consistent with the segregation of single-copies (**Table 3**). In Experiment #5, 5 out of 32 G_0 pupae showed mosaic *3xP3::mCherry* expression (**Table 1**), but these somatic transformants failed to pass a transgene into a G_1 generation, confirming that somatic mosaicism in the pupal eyes is a poor indicator of germline transformation. In contrast, a pooled in-cross of the 17 remaining negative G_0 individuals yielded a high-rate of germline transmission, with 51 out 518 embryos showing strong *3xP3* activity (**Fig. 2C, Table 3**).

In G_1 larvae, we detected *FibL::mBaojin* activity in sections of two inner tubes on either side of the gut, spanning the A3-A6 segments, directly screenable through the cuticle (**Fig. 2C-D, Videos S2**). Dissected glands show that *FibL::mBaoJin* fluorescence is confined to the Posterior Silk Gland (PSG, **Fig. 2F, F'**). This compartment of the silk gland is specialized in the expression of the fibroin genes *FibL* and *FibH* (**Fig. 2F, F'**), and is thus consistent with the *FibL* promoter recapitulating its endogenous expression in *Plodia* (Alqassar et al. 2025). Notably, in G_1 larvae, *FibL* expression in the PSG was also visible when screening with an RFP filter (**Video S3**), suggesting that the *FibL* promoter may be interacting with *mCherry* in addition to *mBaojin*, which could be due to the absence of insulator sequences between the two expression cassettes. G_1 donor successfully established G_2 lines in controlled crosses, including in 4 backcrosses where segregation ratios indicate that a single-insertion allele is present. Even in these G_2 individuals carrying a single-copy of the transgene, fluorescence of both the *mCherry* and *FibL* markers provided extremely bright signals that enable fast screening (**Videos S4-S5**).

Overall, these data further confirm the efficiency of *Minos* transgenesis for a second donor plasmid, and the *FibL::mBaoJin* cassette provides a marker that is easily screenable in *Plodia* throughout the entire larval stage (**Fig. 3A**). The *FibL* promoter could be used in the future to drive the expression of other fluorescent markers or ectopic silk factors in the *Plodia* Posterior Silk Gland.

Discussion

Recommendations for successful transgenesis in *Plodia* and beyond

The feasibility of transgenesis experiments depends not only on the germline integration rate

of the transposase system, but also on other logistic criteria such as the injection, rearing and crossing efforts. Below, we elaborate on these aspects and provide experimental considerations with the overarching goal to facilitate implementation in *Plodia* and other lepidopteran organisms.

We detected lower rates of G_0 mosaic fluorescence with *Minos* compared to previous *HyPBase* experiments, with 9.0% of the G_0 injected eggs and 9.6% of surviving pupae showing a *3xP3*-driven signal, compared to 22% of injected eggs and 32% of surviving pupae with *HyPBase* (Heryanto, Mazo-Vargas, et al. 2022). However, here we established that G_0 injectees devoid of visible somatic activity are effective germline carriers of the transgene. As a consequence, we propose that the random in-crossing of these negative G_0 injectees, performed in pools of adults, offers a practical route to the generation of transgenic lines. For example, in Experiment #1, 341 embryos were microinjected (an effort of only 3 hours for two experimenters). In order to establish a G_1 line, all 14 surviving adults from the injected batch were transferred to a larval diet container and allowed to randomly mate. This approach generated a large proportion of G_1 individuals with *3xP3*-driven fluorescence, with 23.6% of 250 screened pupae showing EGFP expression in their eyes, which were then used to establish two transgenic lines (*EGFP*$^{+}$ and *EGFP*$^{+/oeno}$). In other words, we recommend in-crossing all G_0 individuals to ensure germline transmission and the generation of G_1 transformants. Indeed, crossing of small numbers of G_0 individuals can be time-consuming or yield unsuccessful matings, and selecting G_0 somatic transformants as founders entails the risk that the transgene has not been integrated into the germline. This approach is supported by our results from in-crossing all phenotypically G_0 negative individuals across several experiments, which all resulted in large G_1 cohorts with > 10% transgenic individuals to select from to establish stable lines (**Tables 2, 3**). In contrast, backcrosses of positive G_0 individuals was successful in Experiment #2, but failed to produce any G_1 transformants in Experiment #5.

The pooled G_0 crossing scheme presents some caveats. First, not being able to trace how many individuals reproduced, we could not accurately measure germline integration rates as previously done in other insects, including our report of successful transgenesis in *Plodia* using the *Hyperactive piggyBac* transposase (Gregory et al. 2016; Heryanto, Mazo-Vargas, et al. 2022). With the current data, it is unclear which of the *Minos* or *Hyperactive piggyBac* transposases drives the highest rates of germline transformation. Second, pooling G_0 siblings risks creating G_1 individuals inheriting several insertion sites. While having several insertions segregating in a line is not always an issue, *e.g.* if a transgene is designed to fluorescently label structures for qualitative imaging, or for testing the ability of select promoters to drive tissue specific expression (*e.g.* the *FibL* promoter) , this could be a concern for quantitative or expression-reporter assays that may be influenced by positional effects. In such cases, we recommend sorting G_0 pupae by sex (Heryanto et al. 2025), and mix a pool of G_0 males to an equivalent number of uninjected females, and vice-versa (**Fig. 3B**). Generating a synchronized stock can facilitate this, simply by leaving a portion of the collected embryos uninjected at the beginning of the experiment.

Alternatively, if G_1 broods originate from an in-cross of pooled G_0 siblings, mixing single G_1 transgenic individuals with non-transgenic individuals should generate a majority of G_2 lines where a single transgene insert is segregating. It is worth noting that while we

observed 50% segregation ratios consistent with single-inserts among our G_2-to-G_4 generations (**Tables 2 and 3**), we have not determined whether these lines include transcriptionally silent transgene copies, which might exist if *Minos*-mediated insertions can occur in heterochromatin regions. Inverse/splinkerette PCR or sequencing techniques could be used in the future to map the position of inserts in the genome (Potter and Luo 2010; Pavlopoulos 2011; Stern 2016).

Flexible marker choice using *3xP3* and *FibL* drivers and various fluorophores

The *3xP3:EGFP* and *3xP3:mCherry* markers provide a reliable labeling on larval ocelli, glial tissue, and eyes across insects, including the hemimetabolous crickets and firebrats (Gonzalez-Sqalli et al. 2024; Inada et al. 2025). This signal was strong enough to be screened throughout the cuticle throughout the entire larval stage of the *Plodia wFog* strain, in which a *white* gene null mutation not only results in white eyes but also in increase translucency of the larval cuticle (Heryanto, Hanly, et al. 2022). In species where opaque cuticle may block fluorescence, or where a white-eyed mutant line is not available, it is still be possible to screen for *3xP3* activity in the larval lateral ocelli (Thomas et al. 2002), or in early pupal eyes before melanization occurs (Özsu et al. 2017).

This said, these features make the *3xP3* constraining to use, and we expect *FibL*-driven fluorescence to provide an interesting alternative in some species, particularly those with a reasonably translucent or clear cuticle in the first larval instars. And not only *FibL* may be more convenient to screen, it may also be preferred for experimental reasons, particularly in neurogenetics studies where tagging neural tissues may be undesirable (Fujiwara et al. 2014).

Last, we tested mBaoJin for the first time in a lepidopteran insect, as a monomeric version of the StayGold fluorophores, which show improved photostability and brightness over existing green fluorescent proteins (Zhang et al. 2024; Zhang et al. 2024). Its successful tagging of the silk gland makes it a promising tool as a fusion-protein or expression reporter for Lepidoptera *in-vivo* studies. A plasmid carrying *Minos* repeats, *3xP3:mCherry*, and the *Plodia*-derived *FibL:mBaoJin* marker is available on the Addgene repository for academic use (Addgene #240410).

Conclusions

Our data, together with a previous report in *Bombyx* (Uchino et al. 2007), show that *Minos* transgenesis is applicable to lepidopteran systems, provided it is possible to inject early syncytial embryos and maintain relatively inbred lines. Given the risks of transgene remobilization and instability associated with *piggyBac* transposases of lepidopteran origin, we urge researchers interested in developing transgenesis in moths or butterflies to consider using *Minos*-based tools.

Acknowledgements

We thank Jasmine Alqassar and Christa Heryanto for maintaining *Plodia* cultures, Patricia Hernandez for providing access to microscopy equipment, and the Institutional Biosafety Committee at the George Washington University for administering the approval of *Plodia*

rearing and transgenesis protocols in the Martin lab (protocol #IBC-24-261).

Figures

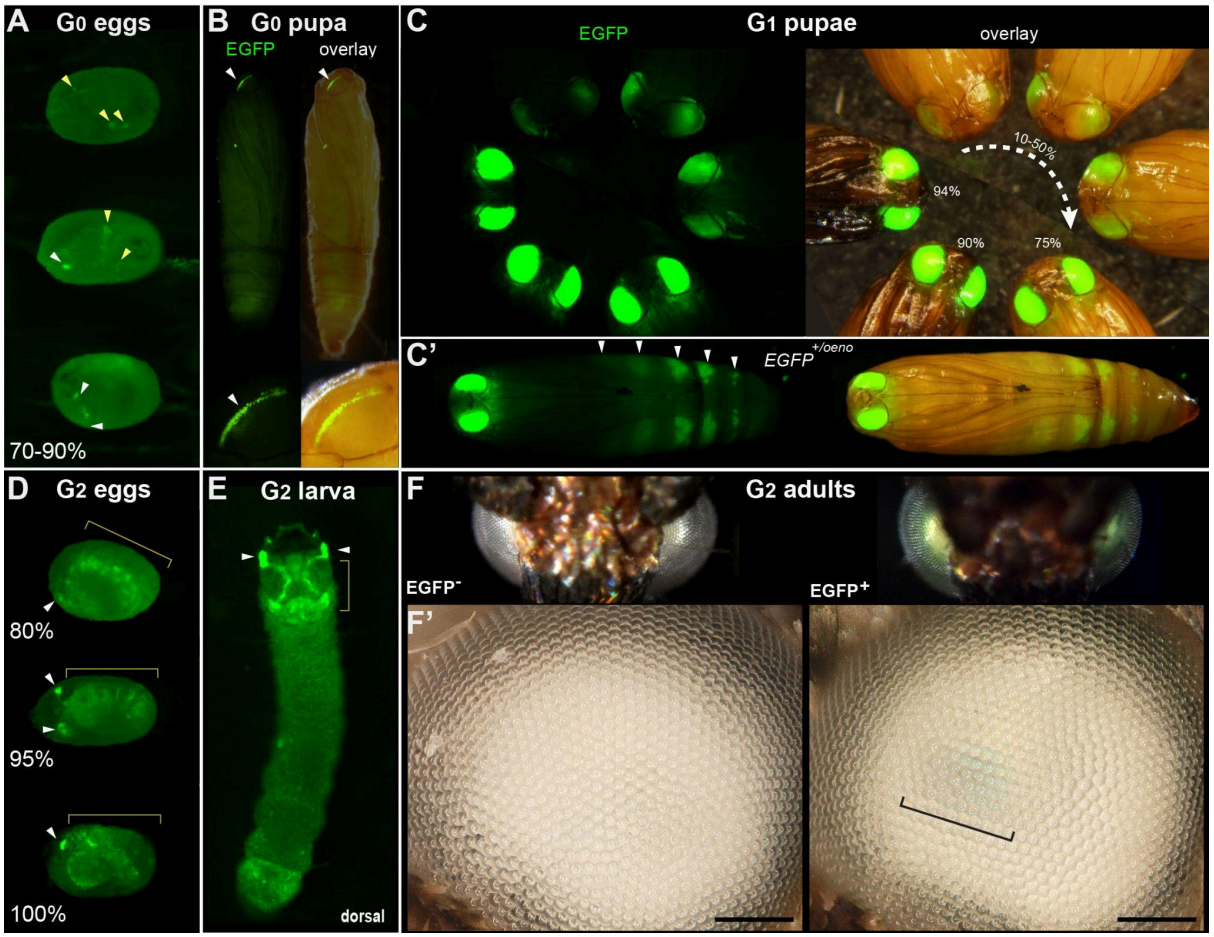

Figure 1. Transgenic *Plodia* carrying the *3xP3::EGFP* cassette via *Minos*-mediated transgenesis. (A) G_0 eggs from injections of the donor plasmid *pMi[3xP3::EGFP]* and *Minos* transposase mRNA. Three examples of *3xP3* activity are shown at 70-90 % of embryonic development. Effects are distinct from uninjected controls (**Fig. S1**). **(B)** Example of a mosaic *3xP3::EGFP* expression in a G_0 pupal eye. Right panels depict an overlay of EGFP and brightfield images taken separately. **(C)** Non-mosaic expression of EGFP in G_1 pupal eyes. EGFP intensity increases with the developmental stage of the pupae. Pupal stages (%) were estimated based on eye, wing, tarsal, and cuticle pigmentation (Zimowska et al. 1991). **(C')** Expression of the *EGFP*$^{+/oeno}$ allele, characterized by ectopic signal in abdominal segments (white arrowheads) in addition to the eyes. This ectopic activity marks oenocytes (**Fig. S2**) and was stable across subsequent generations. **(D)** G_2 embryos show expected *3xP3*::EGFP activity in the developing ocelli and presumptive glia. **(E)** *pMi[3xP3::EGFP]* expression in a first instar G_2 larva shows strong activity in head glia and lateral ocelli. **(F-F')** Adult G_2 individuals positive for *3xP3::EGFP* have green eyes under normal white light, due to strong EGFP expression. Comparison of an G_2 adult negative (left) and positive (right) for *3xP3::EGFP* under white light illumination and without fluorescence filters (F': magnified, lateral views of corresponding eyes). Bracket: visible green tint in inner retina. White arrowheads (A-B, D-E): fluorescent eye/ocelli (white). Yellow arrowheads and brackets (A-B, D-E) : fluorescent glial tissues. Scale bars : F' = 100 µm.

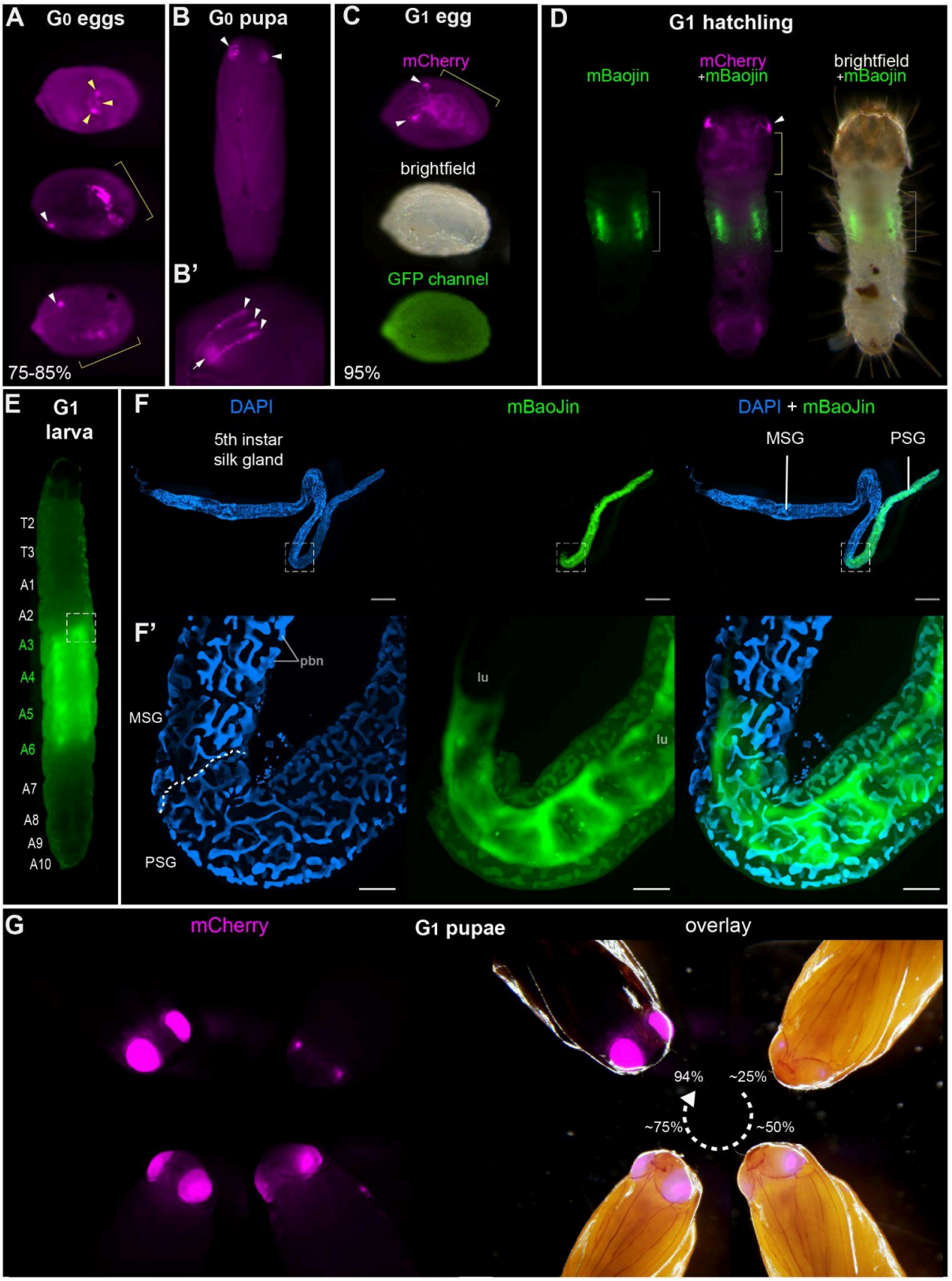
A
G0 eggs
75-85%
B
G0 pupa
B'
C
G1 egg
mCherry
brightfield
GFP channel
95%
D
G1 hatchling
mBaojin
mCherry
+mBaojin
brightfield
+mBaojin
E
G1
larva
T2
T3
A1
A2
A3
A4
A5
A6
A7
A8
A9
A10
F
DAPI
5th instar
silk gland
mBaoJin
DAPI + mBaoJin
MSG
PSG
F'
pbn
MSG
PSG
lu
lu
G
mCherry
G1 pupae
overlay
94%
~25%
~75%
~50%

(previous page) **Figure 2. Tissue-specific activities of the *[3xP3::mCherry, FibL::mBaojin]* transgene following *Minos*-mediated integration. (A)** Mosaic expression of *3xP3::mCherry* in G_0 embryos, following injections of the donor plasmid *pMi[3xP3::mCherry, FibL::mBaojin]* and *Minos* transposase mRNA. Three examples of *3xP3* activity are shown at 75-85% of embryonic development. Arrowheads indicate *3xP3* specific signals in glia and ocelli. **(B-B')** Example of a mosaic *[3xP3::mCherry, FibL::mBaojin]* expression in a G_0 pupal eye. Arrow (B') : deeper non-retinal expression of *3xP3* in the optic lobe. **(C)** Dorsal views a G_1 embryo (95% stage), showing expected *3xP3::mCherry* activity in the developing ocelli and presumptive glia. Brightfield, and autofluorescence in the GFP channel are added underneath. No mBaoJin is detectable in embryos. **(D)** Aspect of *FibL::mBaoJin* green fluorescence in silk glands, directly visible through the dorsal epidermis of a G_1 [*mCherry*+] first instar larva. **(E)** *FibL::mBaoJin* expression in a G_1 fifth instar larva in segments A3-A5. **(F-F')** Dissected silk gland of a G_1 fifth instar larva expressing *FibL::mBaojin* in the Posterior Silk Gland (green). F' panels show confocal stacks of the curved region around the MSG-PSG boundary (dotted line). DAPI counterstaining (blue) highlights polyploid branched nuclei (pbn), in the layer of large cells that surround the gland lumen (lu). The mBaojin signal is strongest in the PSG lumen and extends into the MSG lumen. **(G-G')** Expression of *3xP3::mCherry* in G_1 pupal eyes, increasing with the developmental stage of the pupae (shown as %). White arrowheads (A-D): fluorescent eyes/ocelli. Yellow arrowheads and brackets (A, C-D) : fluorescent glia. Scale bars : F = 500 µm ; F' = 100 µm.

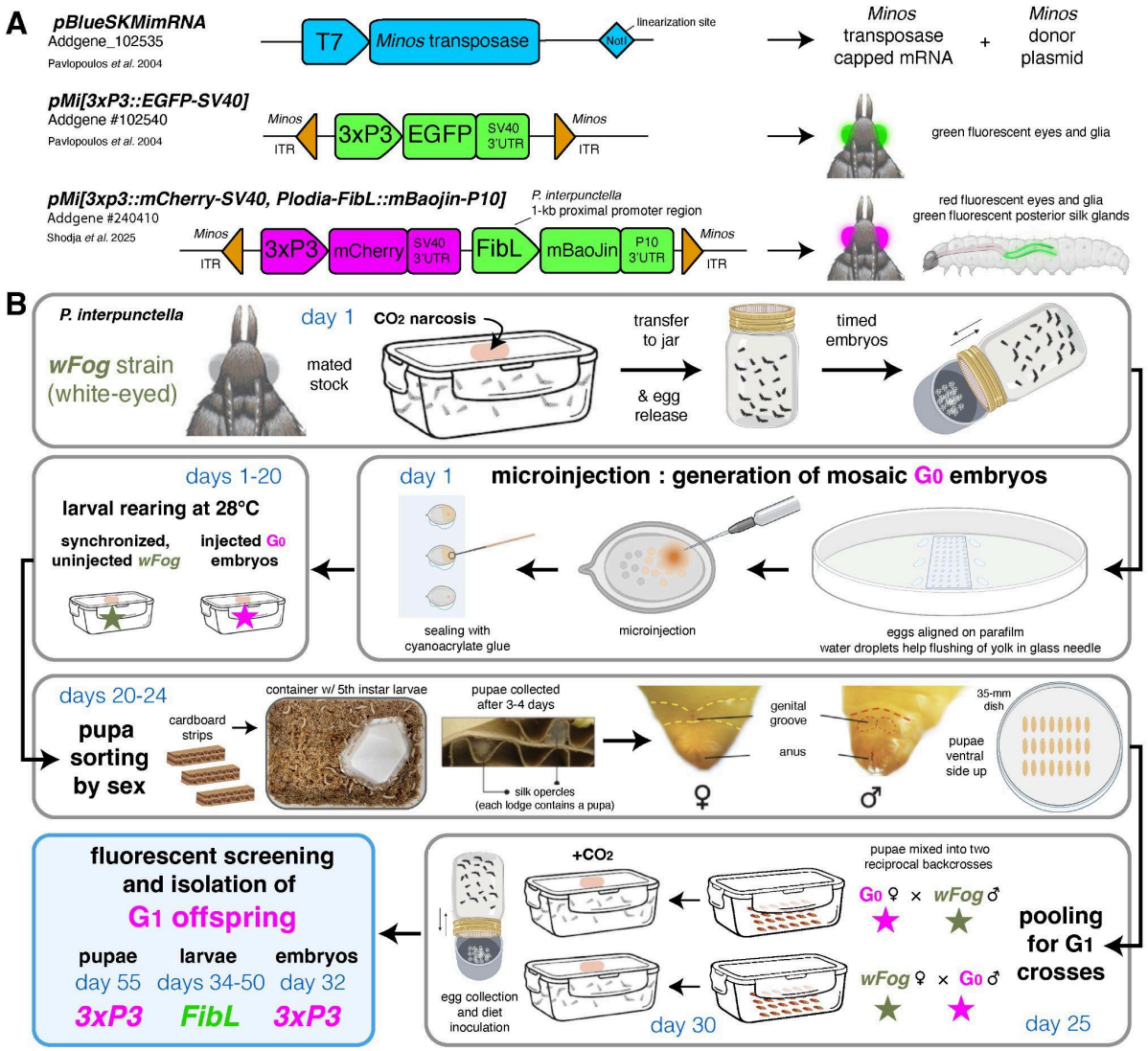

Figure 3. *Minos* transgenesis tools and procedure for the isolation of single-copy G_1 transgenic founders. (A) Plasmids used in this study. **(B)** Suggested procedure for isolating single-copy transgenicheterozygotes at the G_1 generation, using reciprocal back-cross pools of G_0 and uninjected males and females. Alternatively, the G_0 injected stock can be randomly in-crossed if multiple transgene copies are acceptable or preferable, as performed in this study (**Tables 2-3**). Chronology is indicated in days for a 28°C rearing temperature. Full rearing procedures are available online (Heryanto et al. 2025).

Tables

Plasmid	Experiment (injection session)	G_0 embryos			G_0 pupae		
		Injected	*3xP3* somatic transf.	% somatic transf.	Total	*3xP3* somatic transf.	% somatic transf.
pMi[3xP3::EGFP]	**#1**	341	35	10.3%	14	1	7.1%
	#2	696	54	7.8%	51	8	15.7%
	#3	280	12	4.3%	24	4	16.7%
	sub-total	*1317*	*101*	*7.7%*	*89*	*13*	*14.6%*
pMI[3xP3::mCherry, FibL::mBaoJin]	**#4**	456	13	2.9%	77	1	1.3%
	#5	396	82	20.7%	32	5	15.6%
	sub-total	*852*	*95*	*11.2%*	*109*	*6*	*5.5%*
	total	**2169**	**196**	**9.0%**	**198**	**19**	**9.6%**

Table 1. Number of injected embryos and somatic transformation rates among G_0 individuals from Experiments #1-5. Abbreviations — transf. : transformants with detectable *3xP3* activity.

Experiment	Gen.	Cross design	Embryos		Pupae			Chi-2: 50% ratio, single insert
			Total	EGFP+ ocelli & glia	Total screened	EGFP+ eyes	EGFP+ oenocytes	
pMi[3xP3::EGFP] **Experiment #1**	**G_1**	random in-cross of 14 G_0 founders (1 EGFP+, 13 EGFP-, sexes n.d.)	-	-	250	59 (23.6%)	10 (4%)	$p < 0.001$
	G_2	4 ♀ wFog x **1 G_1 [EGFP+]** ♂	-	-	24	17 (70.8%)	0	$p < 0.05$
		1 G_1 [EGFP+] ♀ x 4 G_1 [EGFP-] ♂	-	-	104	70 (67.3%)	0	$p < 0.01$
		4 G_1 [EGFP-] ♀ x **1 G_1 [EGFP+/oeno]** ♂	-	-	80	43 (53.7%)	43 (53.7%)	**n.s.**
		4 G_1 [EGFP-] ♀ x **1 G_1 [EGFP+/oeno]** ♂	-	-	75	40 (53.3%)	n.d. (< 40)	**n.s.**
	G_3	**1 G_2 [EGFP-]** ♀ x 4 wFog ♂	-	-	117	60 (51.3%)	0	**n.s.**
		1 G_2 [EGFP+/oeno] ♀ x 4 wFog ♂	-	-	139	64 (46.0%)	64 (46.0%)	**n.s.**
	G_4	random in-cross of 60 **G_3 [EGFP+]**	-	-	30*	30 (100%)	0	$p < 0.001$
		random in-cross of 64 **G_3 [EGFP+/oeno]**	-	-	70*	70 (100%)	70 (100%)	$p < 0.001$
pMi[3xP3::EGFP] **Experiment #2**	**G_1**	random in-cross of 41 G_0 founders: 29 EGFP- ♀ x 12 EGFP- ♂	470	54 (11.5%)	╳	-	-	$p < 0.001$
		5 G_0 [EGFP+] ♂ x 10 ♀ wFog	113	12 (10.6%)	╳	-	-	$p < 0.001$

Table 2. Cross-design and germline transmission of the *[3xP3::EGFP]* transgene. Only Experiments #1-2 are shown here, as G_0 injectees from Experiment #3 were not crossed to a next generation. The last column indicates the p-value of Chi^2 tests for difference to a 50% distribution. Results are in black for back-crosses to wFog, where a 50% segregation is expected from a single-insertion in the transgenic donors, and greyed out for crosses where a 50% distribution was not expected. Abbreviations — Gen. : generation; n.d. : not determined; n.s. : not significant ($p > 0.05$). Asterisk : number indicates cases where only a fraction of individuals from a line were checked for fluorescence. ╳: these experiments were stopped at the embryonic stage.

Experiment	Gen.	Cross design	Embryos		Larvae			Chi-2: 50% ratio, single insert
			Total	mCher +	Total	mCher+	mBaoJ +	
pMi[3xP3::mCherry, FibL::mBaoJin] **Experiment #4**	**G1**	Random in-cross of 77 G0 founders: 1 mCherry+, 76 mCherry-, sexes n.d.	-	-	n.d. (> 100)	22	22	$p < 0.001$
	G2	4 wFog ☿ x 1 **G1 [mCherry+]** ♂	-	-	0	-	-	
		4 wFog ☿ x 1 **G1 [mCherry+]** ♂	-	-	145	69 (47.5%)	69 (47.5%)	**n.s.**
		1 **G1 [mCherry+]** ☿ x 4 wFog ♂	-	-	242	114 (47.1%)	114 (47.1%)	**n.s.**
		1 **G1 [mCherry +]** ☿ x 4 wFog ♂	-	-	195	94 (48.2%)	94 (48.2%)	**n.s.**
		6 **G1 [mCherry+]** ☿ x 8 **G1 [mCherry+]** ♂			74*	65 (87.8%)	65 (87.8%)	$p < 0.001$
pMi[3xP3::mCherry, FibL::mBaoJin] **Experiment #5**	**G1**	Random in-cross of 27 G0 founders: 13 [mCherry-] ☿ x 14 [mCherry-] ♂	518	51 (9.8%)	╳	-	-	$p < 0.001$
		4 wFog ☿ x 1 **[mCherry+]** ♂	168	0 (0%)	-	-	-	-
		4 **[mCherry+]** ☿ x 7 wFog ♂	160	0 (0%)	-	-	-	-

Table 3. Cross-design and germline transmission of the *[3xP3::mCherry, FibL::mBaoJin]* transgene. The last column indicates the p-value of Chi-square tests of difference to a 50% distribution. Results are in black for back-crosses to *wFog*, where a 50% segregation is expected from a single-insertion in the transgenic donors, and greyed out for crosses where a 50% distribution was not expected. Abbreviations — Gen. : generation; mCher^{+}: mCherry-positive; mBaoJ^{+}: mBaoJin-positive; n.d. : not determined; n.s. : not significant ($p > 0.05$). Asterisk : number indicates cases where only a fraction of individuals from a line were checked for fluorescence. ╳: these experiments were stopped at the embryonic stage.

Supplementary Materials

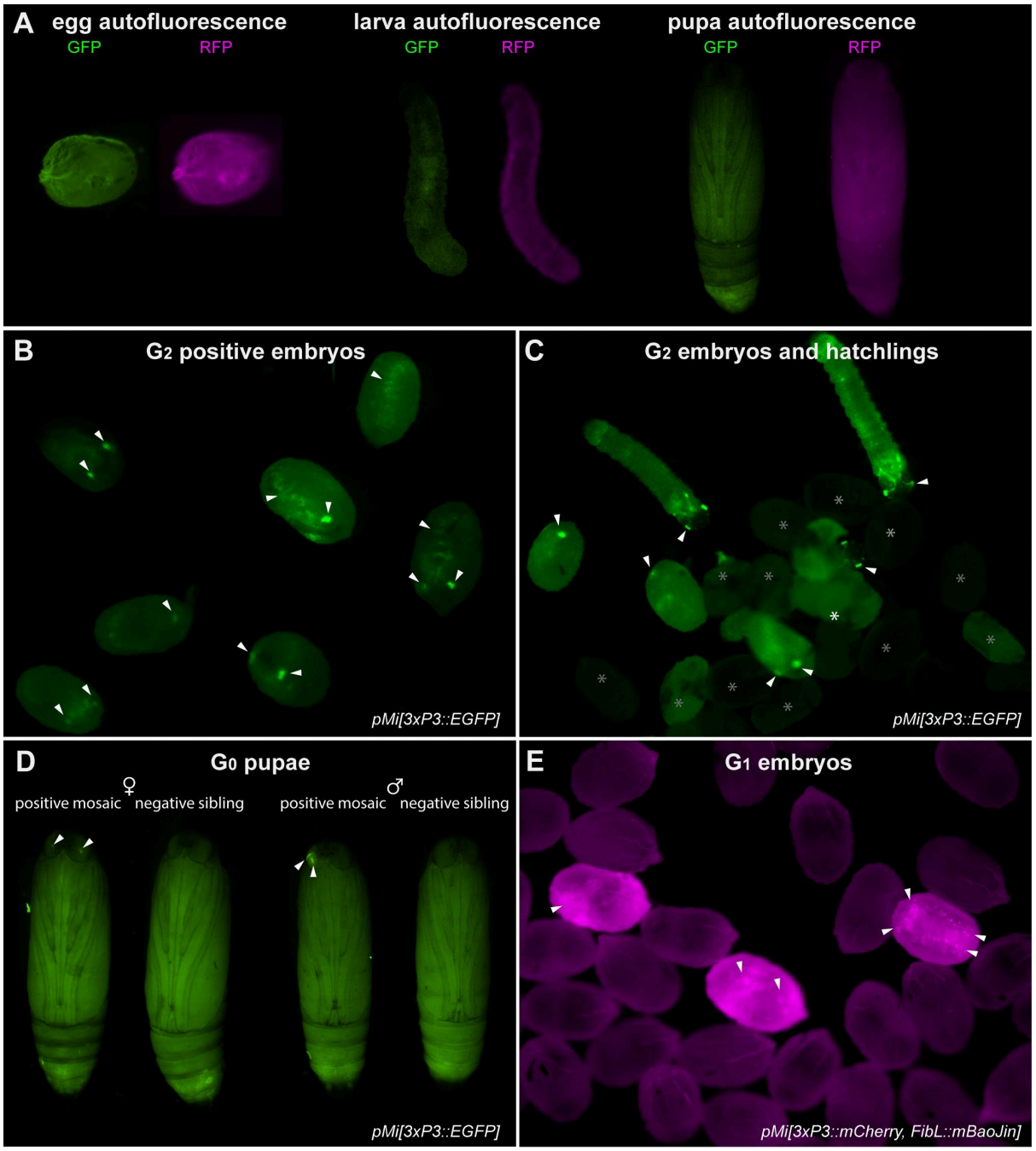

Supplementary Figure 1. Control autofluorescence and fluorescent screening examples. (A) Autofluorescence of an uninjected control egg (left), larva (middle), and pupa (right), imaged under the GFP and RFP filter sets. **(B)** Examples of G_2 embryos positive for *3xP3::EGFP* activity in different orientations (from Experiment #1). **(C)** G_2 embryos and hatchlings positive (arrowheads) and negative (asterisks) for *3xP3::EGFP* activity (from Experiment #1). **(D)** Side by side comparison of G_0 positive mosaics for *3xP3::EGFP* (arrowheads) with their negative siblings, separated by sex. **(E)** G_1 positive (arrowheads) and negative embryos for *3xP3::mCherry* (from in-cross of G_0 negatives from Experiment #5).

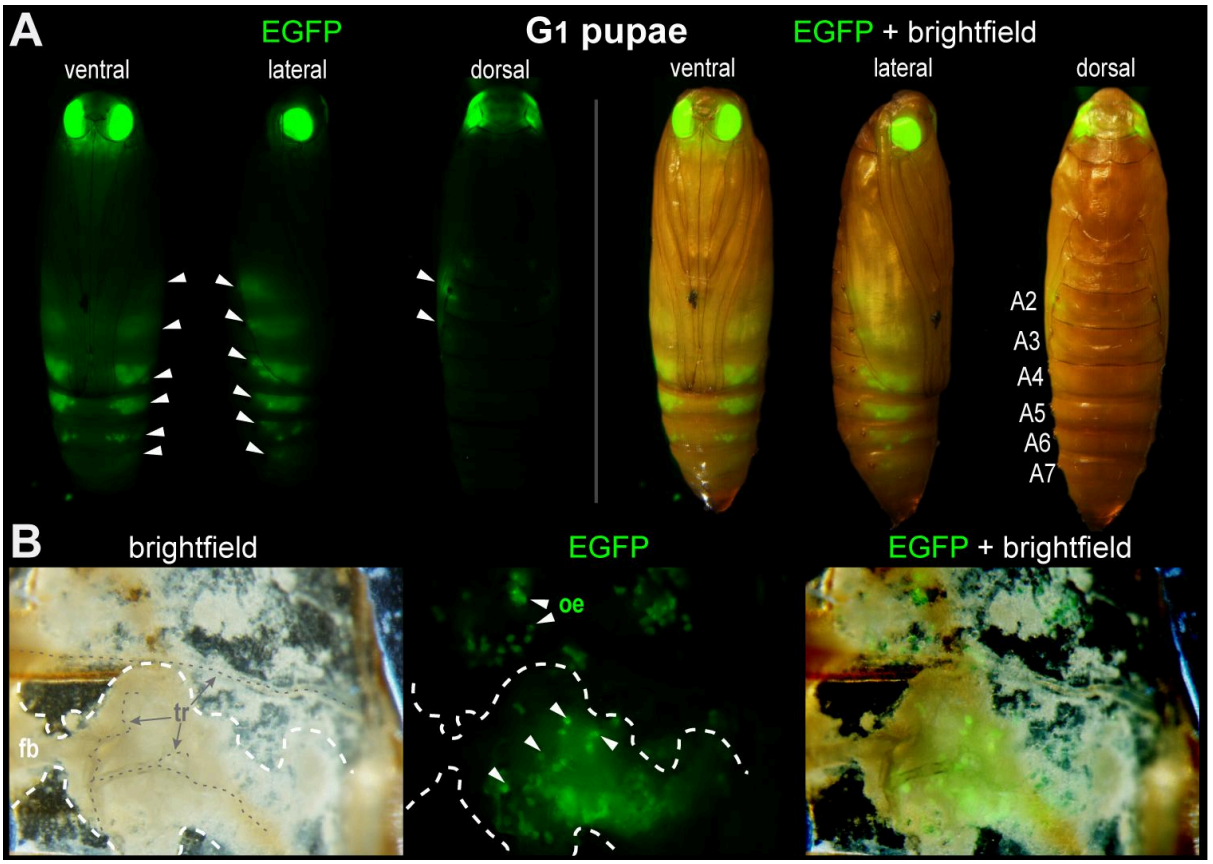

Supplementary Figure 2. A stable transgenic line with ectopic oenocyte expression of *pMi[3xP3::EGFP]* in a portion of G_1 progeny. (A) 10 out of 59 (17%) G_1 pupae positive for *3xP3::EGFP* showed fluorescent activity in metameric belts of cells restricted to the abdominal segments A2 to A7 (white arrowheads). This oenocyte-marking activity, likely derived from a specific insertion site, has been maintained over 3 subsequent generations (G_2–G_4), attesting to the stability of this $EGFP^{+/oeno}$ insertion allele without remobilization. **(B)** Dissection of the pupal cuticle with internal tissues and fat body partially removed. Fluorescence is detected in large cells embedded under the cuticle and in proximity to tracheal projections. These cells have been described as oenocytes in the closely related phycitine moth *Ephestia kuehniella* (Stendell 1912). Abbreviations: tr, trachea ; fb, fat body; oe, oenocytes.

Control experiment	Strain	Embryos		
		Injected/collected	hatched	hatching rate
Mock injection with *pMi[3xP3::EGFP]* (no transposase)	wFog (*white* -/-)	101	13	12.9%
	wFog (*white* -/-)	56	16	28.6%
	total	**157**	**29**	**18.5%**
Positioned on parafilm, uninjected	wFog (*white* -/-)	25	16	64.0%
	wFog (*white* -/-)	302	186	61.6%
	total	**327**	**202**	**61.8%**

Table S1. Control experiments assessing the effect of mock injections on egg hatching rates. Mock injections consisted of injections conditions identical to the transgenesis Experiments #1 to #3, minus the presence of transposase mRNA.

Video S1. Fluorescent detection of the *3xP3::EGFP* transgene in G_2 hatchlings. *pMi[3xP3::EGFP]* fluorescence activity in G_2 first-instar larvae shortly before (left) and during hatching (right), imaged using an EGFP filter set. Shown at real-time speed.

Video S2. Fluorescent detection of the *FibL::mBaojin* marker in a transgenic G_1 hatchling. *FibL::mBaojin* expression in a *pMi[3xP3::mCherry, FibL::mBaojin]* G_1 fifth-instar larva, imaged using an EYFP filter set. Shown at real-time speed.

Video S3. Fluorescent detection of the *3xP3::mCherry* marker in a transgenic G_1 fifth instar larva. *3xP3::mCherry* expression in a *pMi[3xP3::mCherry, FibL::mBaojin]* G_1 fifth-instar larva, imaged using an RFP filter set. Bright expression of *3xP3::mCherry* is detected in the central brain, ocelli, and in isolated ganglia along the body length. Visible expression in the silk glands is likely due to cross-over activity of the *FibL* promoter. Shown at real-time speed.

Video S4. Fluorescent detection of the *FibL::mBaojin* and *3xP3::mCherry* markers in transgenic G_2 larvae. *FibL::mBaojin* (blue/green, GFP filter set) and *3xP3::mCherry* (red, RFP filter set) are shown consecutively at normal speed, followed by a zoom in the RFP channel at 0.3X speed highlighting the expression of mCherry in the larval heads and ocelli.

Video S5. Fluorescent detection of the *FibL::mBaojin* marker in transgenic G_2 larvae. *FibL::mBaojin* (blue/green, GFP filter set) is shown at normal speed across a few larvae to highlight its bright fluorescence and ease of screening.

References

Alqassar JD, Biot M, Eccles LE, Stoppel WL, Martin A. 2025. Regionalization of gene expression and cell types in the silk gland of the pantry moth Plodia interpunctella. :2025.07.11.664249. Available from: https://www.biorxiv.org/content/10.1101/2025.07.11.664249v1

Alqassar JD, Martin A. 2025. Dissection of Plodia silk glands. *Open Science Framework* [Internet]. Available from: https://osf.io/pzshg/

Bossin H, Furlong RB, Gillett JL, Bergoin M, Shirk PD. 2007. Somatic transformation efficiencies and expression patterns using the JcDNV and piggyBac transposon gene vectors in insects. *Insect Molecular Biology* [Internet] 16:37–47. Available from: http://dx.doi.org/10.1111/j.1365-2583.2006.00693.x

Franz G, Savakis C. 1991. Minos, a new transposable element form *Drosophila hydei* is a member of the Tc1-like family of transposons. *Nucl Acids Res* [Internet] 19:6646–6646. Available from: https://academic.oup.com/nar/article-lookup/doi/10.1093/nar/19.23.6646

Fraser MJ, Brusca JS, Smith GE, Summers MD. 1985. Transposon-mediated mutagenesis of a baculovirus. *Virology* [Internet] 145:356–361. Available from: https://linkinghub.elsevier.com/retrieve/pii/0042682285901722

Fujiwara T, Kazawa T, Sakurai T, Fukushima R, Uchino K, Yamagata T, Namiki S, Haupt SS, Kanzaki R. 2014. Odorant Concentration Differentiator for Intermittent Olfactory Signals. *J. Neurosci.* [Internet] 34:16581–16593. Available from: https://www.jneurosci.org/content/34/50/16581

Gonzalez-Sqalli E, Caron M, Loppin B. 2024. The white gene as a transgenesis marker for the cricket Gryllus bimaculatus. *G3 (Bethesda)* 14:jkae235.

Gregory M, Alphey L, Morrison NI, Shimeld SM. 2016. Insect transformation with piggyBac: getting the number of injections just right. *Insect Mol Biol* 25:259–271.

Heryanto C, Hanly JJ, Mazo-Vargas A, Tendolkar A, Martin A. 2022. Mapping and CRISPR homology-directed repair of a recessive white eye mutation in Plodia moths. *iScience*:103885.

Heryanto C, Mazo-Vargas A, Martin A. 2022. Efficient hyperactive piggyBac transgenesis in Plodia pantry moths. *Frontiers in Genome Editing* 4:57.

Heryanto C, Shodja DD, Alqassar JD, Martin A. 2025. A laboratory manual for the rearing, microinjection, and safe handling of the pantry moth Plodia interpunctella. Available from: https://osf.io/bwkgs/

Hozumi A, Kawai N, Yoshida R, Ogura Y, Ohta N, Satake H, Satoh N, Sasakura Y. 2010. Efficient transposition of a single Minos transposon copy in the genome of the ascidian Ciona intestinalis with a transgenic line expressing transposase in eggs. *Dev Dyn* 239:1076–1088.

Imamura M, Nakai J, Inoue S, Quan GX, Kanda T, Tamura T. 2003. Targeted gene expression using the GAL4/UAS system in the silkworm Bombyx mori. *Genetics* 165:1329–1340.

Inada K, Ohde T, Daimon T. 2025. Efficient transgenic system for the firebrat Thermobia domestica utilizing hyPBase and G0 founder prescreening. *Gene* 955:149449.

Jackson EW, Romero E, Kling S, Lee Y, Tjeerdema E, Hamdoun A. 2024. Stable germline transgenesis using the Minos Tc1/mariner element in the sea urchin Lytechinus pictus. *Development* 151:dev202991.

Jia X, Pang X, Yuan Y, Gao Q, Lu M, Zhang G, Dai F, Zhao T. 2021. Unpredictable recombination of PB transposon in Silkworm: a potential risk. *Mol Genet Genomics* 296:271–277.

Kapetanaki MG, Loukeris TG, Livadaras I, Savakis C. 2002. High frequencies of Minos transposon mobilization are obtained in insects by using in vitro synthesized mRNA as a source of transposase. *Nucleic acids research* 30:3333–3340.

Khurana JS, Wang J, Xu J, Koppetsch BS, Thomson TC, Nowosielska A, Li C, Zamore PD, Weng Z, Theurkauf WE. 2011. Adaptation to P element transposon invasion in Drosophila melanogaster. *Cell* 147:1551–1563.

Kontarakis Z, Pavlopoulos A. 2014. Transgenesis in non-model organisms: the case of Parhyale. *Methods Mol Biol* 1196:145–181.

Kuo D-H, Szczupak L, Weisblat DA, Portiansky EL, Winchell CJ, Lee J-R, Tsai F-Y. 2024. Transgenesis enables mapping of segmental ganglia in the leech Helobdella austinensis. *Journal of Experimental Biology* 227:jeb247419.

Loukeris TG, Arcà B, Livadaras I, Dialektaki G, Savakis C. 1995. Introduction of the transposable element Minos into the germ line of Drosophila melanogaster. *Proc Natl Acad Sci U S A* 92:9485–9489.

Makki R, Cinnamon E, Gould AP. 2014. The Development and Functions of Oenocytes. *Annu Rev Entomol* [Internet] 59:405–425. Available from: https://www.ncbi.nlm.nih.gov/pmc/articles/PMC7613053/

Metaxakis A, Oehler S, Klinakis A, Savakis C. 2005. Minos as a genetic and genomic tool in Drosophila melanogaster. *Genetics* 171:571–581.

Moon S, Cassani M, Lin YA, Wang L, Dou K, Zhang ZZ. 2018. A Robust Transposon-Endogenizing Response from Germline Stem Cells. *Dev Cell* 47:660-671.e3.

Pavlopoulos A. 2011. Identification of DNA sequences that flank a known region by inverse PCR. *Methods Mol Biol* 772:267–275.

Pavlopoulos A, Berghammer AJ, Averof M, Klingler M. 2004. Efficient transformation of the beetle Tribolium castaneum using the Minos transposable element: quantitative and qualitative analysis of genomic integration events. *Genetics* 167:737–746.

Pearce JC, Campbell JS, Prior JL, Titball RW, Wakefield JG. 2024. PiggyBac mediated transgenesis and CRISPR/Cas9 knockout in the greater waxmoth, Galleria mellonella. :2024.09.17.613535. Available from: https://www.biorxiv.org/content/10.1101/2024.09.17.613535v1

Potter CJ, Luo L. 2010. Splinkerette PCR for mapping transposable elements in Drosophila. *PloS one* [Internet] 5:e10168. Available from:

https://journals.plos.org/plosone/article?id=10.1371/journal.pone.0010168

Shim J-K, Lee K-Y. 2015. Chilling results in failure of silk secretion by wandering larvae of *Plodia interpunctella*. *Journal of Asia-Pacific Entomology* [Internet] 18:483–487. Available from: https://www.sciencedirect.com/science/article/pii/S1226861515000680

Shirk BD, Shirk PD, Furlong RB, Scully ED, Wu K, Siegfried BD. 2023. Gene editing of the ABC Transporter/White locus using CRISPR/Cas9-mediated mutagenesis in the Indian Meal Moth. *J Insect Physiol* 145:104471.

Shirk PD, Zimowska G. 1997. An α-crystallin protein cognate in germ cells of the moth, *Plodia interpunctella*. *Insect Biochemistry and Molecular Biology* [Internet] 27:149–157. Available from: https://www.sciencedirect.com/science/article/pii/S0965174896000793

Stendell W. 1912. Beiträge zur Kenntnis der Oenocyten von Ephestia kuehniella Zeller. *Zeitschrift für wissenschaftliche Zoologie* [Internet] 102:137–168. Available from: https://cir.nii.ac.jp/crid/1130282268969539584

Stern DL. 2016. Tagmentation-based mapping (TagMap) of mobile DNA genomic insertion sites. *BioRxiv* [Internet]:037762. Available from: https://www.biorxiv.org/content/10.1101/037762.abstract

Teixeira FK, Okuniewska M, Malone CD, Coux R-X, Rio DC, Lehmann R. 2017. piRNA-mediated regulation of transposon alternative splicing in the soma and germ line. *Nature* 552:268–272.

Thomas JL, Da Rocha M, Besse A, Mauchamp B, Chavancy G. 2002. 3xP3-EGFP marker facilitates screening for transgenic silkworm Bombyx mori L. from the embryonic stage onwards. *Insect Biochem Mol Biol* 32:247–253.

Uchino K, Imamura M, Shimizu K, Kanda T, Tamura T. 2007. Germ line transformation of the silkworm, Bombyx mori, using the transposable element Minos. *Molecular Genetics and Genomics* 277:213–220.

Wang F, Wang R, Wang Y, Xu H, Yuan L, Ding H, Ma S, Zhou Y, Zhao P, Xia Q. 2015. Remobilizing deleted piggyBac vector post-integration for transgene stability in silkworm. *Mol Genet Genomics* 290:1181–1189.

Wang J, Miller ED, Simmons GS, Miller TA, Tabashnik BE, Park Y. 2010. piggyBac-like elements in the pink bollworm, Pectinophora gossypiella. *Insect Mol Biol* 19:177–184.

Wu M, Sun Z, Hu C, Zhang G, Han Z. 2008. An active *piggyBac* -like element in *Macdunnoughia crassisigna*. *Insect Science* [Internet] 15:521–528. Available from: https://onlinelibrary.wiley.com/doi/10.1111/j.1744-7917.2008.00241.x

Xu X, Harvey-Samuel T, Siddiqui HA, Ang JXD, Anderson ME, Reitmayer CM, Lovett E, Leftwich PT, You M, Alphey L. 2022. Toward a CRISPR-Cas9-Based Gene Drive in the Diamondback Moth Plutella xylostella. *CRISPR J* 5:224–236.

Zagoraiou L, Drabek D, Alexaki S, Guy JA, Klinakis AG, Langeveld A, Skavdis G, Mamalaki C, Grosveld F, Savakis C. 2001. In vivo transposition of Minos, a Drosophila mobile element, in mammalian tissues. *Proc Natl Acad Sci U S A* 98:11474–11478.

Zhang H, Lesnov GD, Subach OM, Zhang W, Kuzmicheva TP, Vlaskina AV, Samygina VR, Chen L, Ye X, Nikolaeva AY, et al. 2024. Bright and stable monomeric green fluorescent protein derived from StayGold. *Nat Methods* 21:657–665.

Zimowska G, Silhacek DL, Shaaya E, Shirk PD. 1991. Immuno-Fluorescent analysis of follicular growth and development in whole ovaries of the Indianmeal moth. *J Morphol* 209:215–228.

Zimowska GJ, Handler AM. 2006. Highly conserved piggyBac elements in noctuid species of Lepidoptera. *Insect biochemistry and molecular biology* [Internet] 36:421–428. Available from: https://www.sciencedirect.com/science/article/pii/S096517480600052X?casa_token=auVJJxD9TacAAAAA:C1qPTU9hWilo00Tix1N8GE8VnDsyzLNBlf0AJ-tz1WlecipHoTW-qEJbwPb6Legbg6ePOJA